

HYDROGEN-ASSISTED FAILURE OF ALLOYS X-750 AND 625 UNDER SLOW STRAIN-RATE CONDITIONS

R.S. Daum, A.T. Motta, D.A. Koss, and D.D. Macdonald

The Pennsylvania State University
University Park, PA 16802

Abstract

Slow strain-rate tensile testing of Ni-based Alloys X-750 and 625 was performed in high-purity, deaerated water in order to determine whether hydrogen embrittlement occurs in these alloys at room temperature and 288°C. These tests were conducted at an initial strain-rate of 4.6×10^{-7} /sec under both 30 psig nitrogen (0 cc H₂/kg H₂O STP) and 40 psig hydrogen (60 cc H₂/kg H₂O STP), on Alloy X-750 in two heat-treatment conditions and on Alloy 625 in a direct aged condition. At room temperature in the hydrogenated environment, both alloys showed a pronounced susceptibility to hydrogen embrittlement. The presence of hydrogen reduced both the elongation to failure and the reduction in area at fracture by about 50%. Fractography indicated a transition from ductile, transgranular failure in the nitrogen environment to predominantly intergranular fracture under hydrogenated conditions. Fractography of the specimens tested at room temperature showed a transition in crack growth behavior from mixed mode slip band decohesion in nitrogen environments to Mode I intergranular fracture path in hydrogenated environments. In contrast, hydrogen had no effect on the measured properties at 288°C.

Introduction

Materials used as reactor internals require unique properties for both low- and high-temperature service. In particular, in some light water reactor (LWR) applications, components such as fasteners, support beams, springs, and control rod guide pins, require high strength and good resistance to both corrosion and irradiation damage. The nickel-base Alloy X-750 is commonly used in such applications. Although Alloy X-750 and other high-strength nickel-base alloys have performed well in LWR environments, a number of failures have been observed due to intergranular stress corrosion cracking (IGSCC) after long reactor exposures¹⁻⁴. A characteristic of IGSCC in nickel-base alloys is the transition from a ductile, transgranular fracture mode outside the reactor environment to a predominantly brittle, intergranular fracture mode in the aggressive reactor environment¹⁻³. Such problems have prompted a search for alternate alloys, such as the nickel-base Alloys 625 and 718.

Initially, the nuclear power industry followed the treatment for Alloy X-750 developed by the aerospace industry^{5,6}. This heat treatment (designated as the AH heat treatment) consisted of a stress-equalizing anneal (885°C) for 24 hours and aging (704°C) for 20 hours. This material showed great susceptibility to IGSCC⁷⁻⁹ and hydrogen embrittlement (HE)⁸⁻¹⁰. An alternate heat treatment, designated HTH, was then developed to overcome the short comings of the AH material. The HTH heat treatment consisted of a solution anneal at 1093°C for 1 to 2 hours followed by aging at 704°C for 20 hours. The final HTH material had larger grain size (100-120µm), finer γ' -precipitation, and semi-continuous intergranular carbide precipitation⁸⁻¹¹. The enhanced IGSCC resistance of the HTH material was attributed to the semi-continuous intergranular carbides rather than the discrete intergranular carbide precipitation found in the AH material^{8-10,12}.

Despite the better properties of the HTH material, premature failures still occurred with intergranular fracture paths, causing the industry to examine the stress corrosion cracking performance in hydrogenated environments of other high-strength alloys, such as the nickel-base Alloy 625. Originally, the strength of Alloy 625 was achieved by solid solution-strengthening through additions of Mo and Nb. However, industry researchers found that a precipitation heat treatment imparted irradiation-assisted stress corrosion cracking resistance similar or superior to that of the X-750 HTH material over all relevant ranges of temperature^{13,14}. Direct aging (DA) of hot rolled Alloy 625 at 663°C for 80 hours resulted in uniform precipitation of fine (15nm), disc-shaped γ'' -particles [Ni₃(Nb,Ti,Al)] and large transgranular (Nb,Ti)CN carbonitrides¹⁴. In the solid solution-strengthened heat treatment (usually 1066°C for 1 hour), precipitation was limited to discrete (Nb,Ti)C-type carbides in the grains and grain boundaries¹⁵⁻¹⁷.

One strategy to mitigate the alloy susceptibility to IGSCC involves the establishment of a reducing environment by maintaining an appropriate concentration of dissolved hydrogen in the LWR coolant. This strategy accomplishes three primary tasks^{1,2}: (1) it suppresses radiolysis, and hence lowers the concentrations of highly oxidizing species, such as H₂O₂ and OH, (2) it lowers the concentration of dissolved oxygen entrained with the feedwater, and (3) it lowers the electrochemical potential of the alloy, which reduces the crack growth rate. However, hydrogen has also been found to promote embrittlement in nickel-

base alloys^{18,19}, leading to a decreases in ductility and hence to the premature failure of components.

Previous studies showed that nickel-base alloys that have been exposed to H₂-gas sources^{7-10,12,13,20} or hydrogen by precharging^{15,16,21-23}, show a significant decrease in ductility accompanied by an increase in intergranular fracture at temperatures below 150°C. However, these studies indicate that the effect of hydrogen is less at temperatures greater than 280°C as compared to the low temperature regime. Nonetheless, 30-60% reductions in the elongation to failure and reduction in area of both Alloys X-750^{7-10,12,22} and 625^{15,16} have been measured within these temperature ranges when these materials contain approximately 10 atom percent hydrogen in solution. Also, a significant increase (orders of magnitude) in intergranular crack growth rates has accompanied these reductions in tensile ductility^{1-3,8-10,12,15,16,22}.

This study investigated the relative susceptibilities of Alloy X-750, in the AH and HTH thermally treated conditions, and the direct-aged nickel-base Alloy 625 to hydrogen embrittlement (HE) under simulated (out-of-flux) LWR conditions. We have determined the extent of hydrogen embrittlement as a function of temperature, utilizing specimen elongation to failure, reduction in area, and total intergranular fracture observed, under SSRT testing conditions. Extending the previous research on these alloys, we examined the hydrogen-induced surface cracking and related this behavior to the loss of ductility measurements.

Experimental Procedures

Material

Commercial heats of the nickel-base Alloys X-750 and 625 were obtained for this study from Inco Alloys International and Carpenter Technology Corporation in the form of 0.25 inch (0.635 cm) round bar stock. The compositions of these heats are given in Table I.

Table I As-received Alloy Compositions (in weight percent)

ELEMENT	X-750	625
NICKEL	72.8	62.2
CHROMIUM	15.7	21.9
MOLYBDENUM	-	8.74
IRON	7.07	2.53
NIوبيUM + TANTALUM	0.9	3.87
TITANIUM	2.5	0.28
COBALT	0.09	0.04
ALUMINUM	0.71	0.2
MANGANESE	0.06	0.03
COPPER	0.02	-
SILICON	0.11	0.1
CARBON	0.05	0.04
SULFUR	< 0.001	< 0.001
PHOSPHORUS	-	0.004
BORON	-	-

The Alloy X-750 heat was processed by electroslag remelting and vacuum induction melting methods, followed by a stress equalization treatment at 885°C (1625°F) for 24 hours. The Alloy 625 heat was solution annealed at 1010°C (1850°F) for 1 hour. After machining of the tensile specimens, the alloys were then heat-treated in a dynamic vacuum of $\leq 5 \times 10^{-8}$ torr, as indicated in Table II.

Table II Heat Treatments

Alloy Designation	Annealing Step	Aging Step
X-750¹ HTH	1076°C (1968°F) 1 hr (VC)	704°C(1300°F) 20 hrs (VC)
X-750¹ AH	-	704°C(1300°F) 20 hrs (VC)
625² DA	-	663°C(1225°F) 80 hrs (VC)

¹denotes that Inco stress-equalized at 885°C (1625°F) for 24 hrs
²denotes that Carpenter solution-annealed at 1010°C (1850°F) for 1 hr
 VC = Vacuum Cooled

The microstructures of X-750 HTH, X-750 AH, and 625 DA were characterized by both light and scanning electron microscopies (SEM) in order to evaluate carbide distributions. Metallography samples were etched for 20 seconds using a solution of 4g CuCl₂, 40ml HCl, 40ml methanol, and 40ml H₂O.

Slow Strain-rate Test (SSRT) System

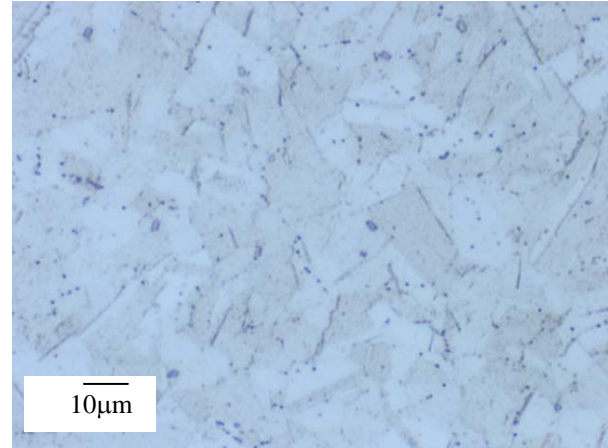
Slow strain-rate tensile specimens were machined from the round bar stock in accordance with ASTM Standard E8-96a. The original gage section dimensions were 0.8 inch (2.032cm) length and 0.125 inch (0.318cm) diameter, with ± 0.005 inch tolerances. A series of four high pressure and temperature autoclaves were connected to a motor-driven constant extension rate device in a manner similar to that described by Macdonald²⁴ and Skeldon et al^{10,25}. A combination of a motor, variable reduction gearing, and a linear actuator produced an initial nominal strain-rate for the SSRT specimens of 4.6×10^{-7} /sec.

The testing environment consisted of a high-purity, deaerated water with either dissolved nitrogen (0 psig hydrogen) or hydrogen (40 psig H₂) overpressure. These conditions resulted in test environments which contain either no dissolved H₂ (30 psig N₂) or 60 cc H₂/kg H₂O STP, using Henry's Law. The solution pH, measured at ambient temperature, was maintained between 10.0 and 10.3. Conductivity and dissolved oxygen gas were maintained at levels below 100 μ S/cm and 10ppb, respectively. The hydrostatic pressure of the system was maintained at 2000-2100 psi and the flow rate was set at 3.5 liters/hour. The system temperature was controlled to within $\pm 5^\circ$ C over the temperature range of 26°C (75°F) to 288°C (550°F). The loads of four specimen cells, solution pH, conductivity, and dissolved oxygen were automatically monitored and saved to disk.

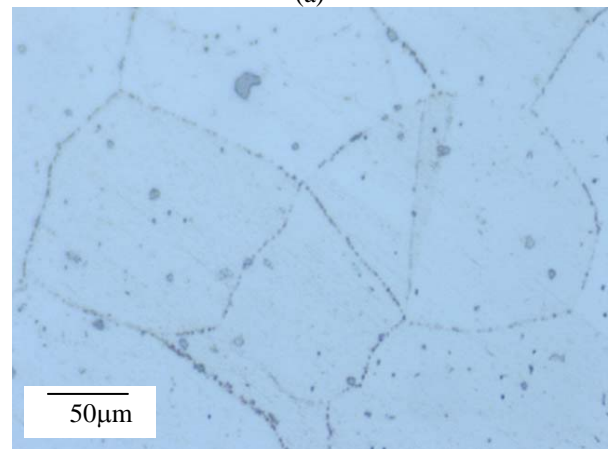
Results and Discussion

Material

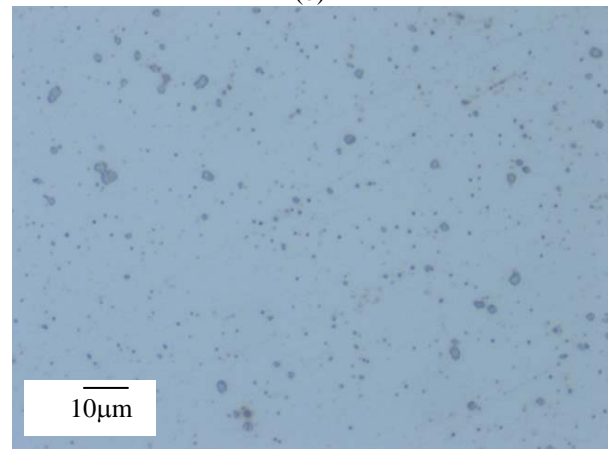
Figure 1 shows the carbide distributions of Alloy X-750 in both the HTH and AH conditions and Alloy 625 in the direct-aged (DA) condition. Figure 1(a) shows the microstructure of the AH



(a)



(b)



(c)

Figure 1: Micrographs of carbide formation for (a) X-750 AH, (b) X-750 HTH, and (c) 625 DA

material, which reveals a 12-15 μm grain size but little intergranular carbide precipitation. Figure 1(b) shows semi-continuous carbide precipitation on the grain boundaries of the HTH material, which has a 110 μm grain size. Alloy 625 DA (grain size not evaluated) shows only large globular intragranular carbides, similar to the “matrix” carbides of the X-750 materials. The hardnesses of heat treated X-750 AH, X-750 HTH, and 625 DA on a Rockwell C scale were found to be 36.5, 35.5, and 44, respectively.

SSRT Results

The relative hydrogen embrittlement susceptibilities of the AH, HTH, and DA materials were assessed and compared by measuring the tensile strength, failure time, elongation to failure, and reduction in area at fracture in both the nitrogenated and hydrogenated environments. As shown by the tensile data of Figure 2, all three materials show a severe reduction in failure time at room temperature. This is consistent with the low-temperature embrittlement of these alloys as reported by others^{7-10,12,22,25}.

In contrast, at 288 $^{\circ}\text{C}$, the hydrogen tests (60 cc H₂/kg H₂O) are indistinguishable from the nitrogen tests (0 cc H₂/kg H₂O).

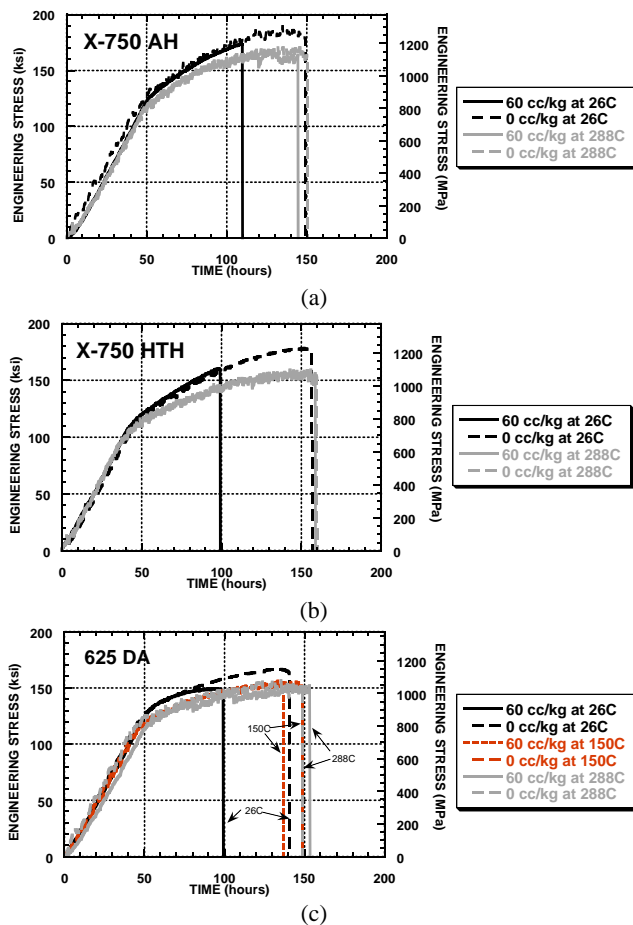


Figure 2: Engineering stress versus time response for Alloys (a) X-750 AH, (b) X-750 HTH, and (c) 625 DA

Figure 2 shows that the tensile strength decreases with increasing temperature, as is characteristic of nickel-base Alloy X-750¹⁰. Regardless of heat treatment and temperature, there appears to be no effect of hydrogen on the yield and flow stresses of Alloy X-750. However, as shown in Figure 2(c), Alloy 625 DA shows a lower flow stress at large strains in the room temperature hydrogenated tests. As will be discussed later, this effect is a result of surface crack growth, which decreases the load-bearing capacity of the material.

The hydrogen embrittlement susceptibility of these materials is summarized in Figure 3 by normalizing the ultimate tensile strength and failure times in the hydrogenated environment to those of the nitrogenated environment; i.e. we plotted the ultimate tensile strength (UTS) ratios ($UTS_{60 \text{ cc H}_2/\text{kg H}_2\text{O}}/UTS_{0 \text{ cc H}_2/\text{kg H}_2\text{O}}$) and the failure time ratios ($t_{60 \text{ cc H}_2/\text{kg H}_2\text{O}}/t_{0 \text{ cc H}_2/\text{kg H}_2\text{O}}$). For the materials examined, Figure 3(a) shows less than a 15% reduction in UTS due to hydrogen for tests at room temperature. On the other hand, at higher temperatures, the reduction in UTS is roughly 5% for all three materials, indicating that hydrogen influences the strength of these materials only slightly. These results are similar to those of Miglin and Domian⁸ who reported less than a 10% reduction in UTS for Alloy X-750 in both the AH and HTH condition for temperatures less than 340 $^{\circ}\text{C}$.

As stated previously, the failure times (Figure 3(b)) at room temperature are severely reduced by the presence of hydrogen in

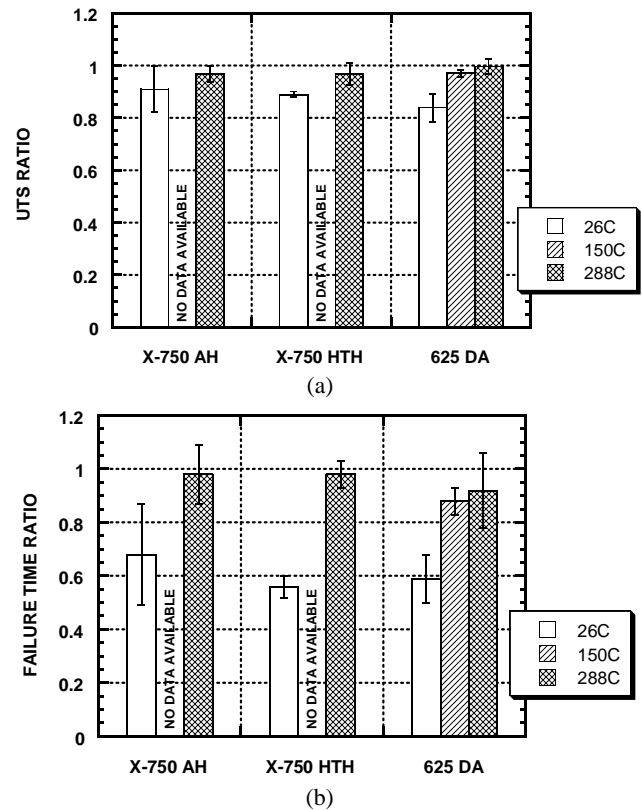


Figure 3: Normalized ratio of (a) UTS and (b) failure time under hydrogenated to nitrogenated conditions as a function of testing temperature and material.

the environment. Specifically, the failure times decrease by about 33, 45, and 40% for the AH, HTH, and DA materials, respectively. Finally, the data for Alloy 625 DA in Figure 3 shows only a minor degree of hydrogen embrittlement susceptibility at 150°C, as indicated by the 3 and 15% reductions in UTS and failure time, respectively. Under similar testing conditions, Skeldon and Hurst^{10,25} reported 56 and 60% reductions in the failure time for Alloy X-750 AH and Alloy X-750 HTH, respectively, when comparing tests at 50°C in pure helium gas and in a PWR water solution hydrogenated to 50 cc H₂/kg H₂O STP; thus, our data suggests somewhat less embrittlement.

Figure 4 shows that the post-fracture evaluations of elongation to failure and reduction in area at fracture indicate a significant reduction in ductility for all materials when tested in ambient temperature hydrogenated water. All of our materials show about a 50-60% reduction in elongation to failure and reduction of area at fracture when tested in hydrogenated environments at room temperature as compared to the non-hydrogenated cases. In an extreme case, Symons²² measured reductions of 65% and 90% in the elongation to failure for X-750 HTH tensile specimens precharged with hydrogen to 5.7 and 65 wppm, respectively, as compared to the as-received materials. Conversely, this study finds no discernible hydrogen effect for all materials tested at 288°C. However, Alloy 625 DA shows a

roughly 30% decrease in the reduction in area at fracture when evaluated at 150°C, suggesting susceptibility to hydrogen embrittlement at intermediate temperatures.

Taken together, the SSRT data indicates roughly equal susceptibilities to hydrogen embrittlement for Alloy X-750 in the AH and HTH conditions and for Alloy 625 in the DA condition for our particular test conditions. The approximate 50% decrease in ductility found at room temperature, as compared to higher temperatures, is consistent with the reported low temperature ductility of these three materials in hydrogenated environments^{8,10,13,15,22}.

Fractography and Surface Cracking

The room temperature failure of all materials tested under hydrogenated conditions in this study followed an intergranular fracture path, as shown in Figure 5. No intergranular fracture was observed at room temperature in nitrogenated environments for any of the alloys. In all the materials, the intergranular fracture path extends from the specimen surface to the interior, which is consistent with surface crack initiation and subsequent propagation. Fractographic analyses of the projected area of intergranular fracture present on the total cross section of the failed specimens indicate that, at ambient temperature, all materials exhibit approximately 15% intergranular fracture. As reported by other researchers^{9,10,15,16}, the room temperature fracture path is consistent with the low temperature hydrogen embrittlement susceptibility of these alloys.

In contrast, in the 288°C hydrogenated tests, the X-750 AH and HTH materials exhibit no intergranular failure, as seen in previous work at temperatures $\geq 250^\circ\text{C}$ ^{8-10,12}. We observed ductile, transgranular failure (by microvoid initiation, growth, and coalescence), which initiated near the central axis of the specimen. This damage accumulated until the load-bearing capacity of the material was exceeded and final fracture occurred by shear, consistent with the cup-cone type fracture morphology. However, other than the severe intergranular fracture associated with the room temperature hydrogenated tests, only a limited amount of grain boundary separation (amounting to less than 3% intergranular fracture) was observed in the HTH material tested under all other conditions. Alloy 625 DA failed by complete 45° shear under 150°C and 288°C hydrogenated conditions; there was no evidence of intergranular fracture.

The SSRT specimen surfaces for the three materials examined also show an increased amount of surface crack formation when tested at ambient temperature under hydrogenated conditions. These cracks appeared to propagate in a Mode I manner on a plane normal to the stress axis and with large Mode I crack opening displacements, as seen in Figures 6(a) and 6(b) (arrow indicates loading direction). Alloy 625 DA showed the greatest amount of surface cracking. The growth of these cracks results in the time-dependent decrease in flow stress evident in Alloy 625 DA when exposed to hydrogen at room temperature. The propagation of the Mode I cracks also generates a direct path for hydrogen ingress into the center of the specimen. This would explain the large extent of intergranular fracture near the central axis of the specimen. Hertzberg and Was²⁶ reported approximately a factor of 10 increase in the surface crack density (cracks/mm²) of controlled-purity Alloy 600 tested in

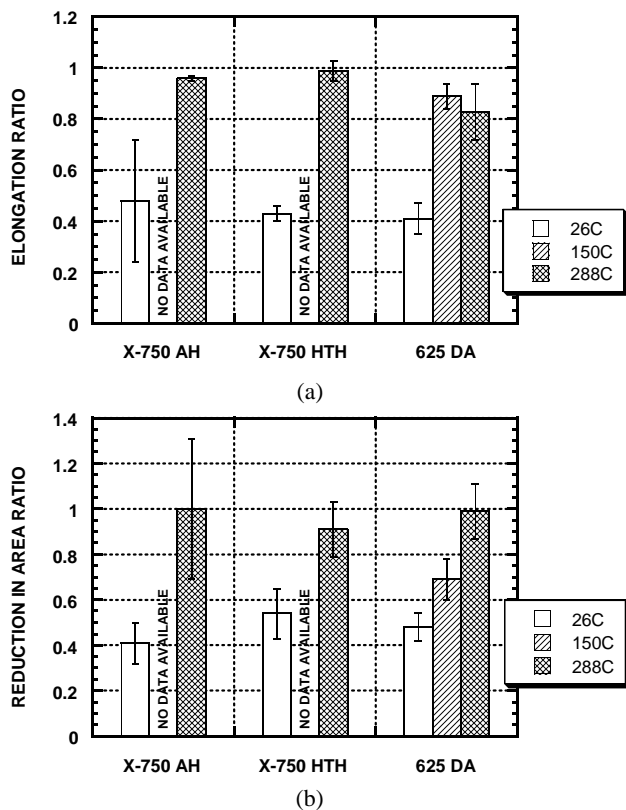


Figure 4: Normalized ratio of (a) elongation to failure and (b) reduction in area at fracture under hydrogenated conditions to nitrogenated conditions as a function of testing temperature and material.

both non-hydrogenated and hydrogenated PWR water at 360°C. They also reported measuring a four-fold increase in surface crack depth for specimens tested in hydrogenated water compared to non-hydrogenated water. Although this report indicates that Alloy 600 suffers from high temperature hydrogen embrittlement, simply increasing the dissolved hydrogen gas content of the environment leads to large increases in surface cracking. Figures 6(a) and 6(c) show this increasing surface cracking characteristic of Alloys X-750 and 625 under both room temperature hydrogenated and nitrogenated testing

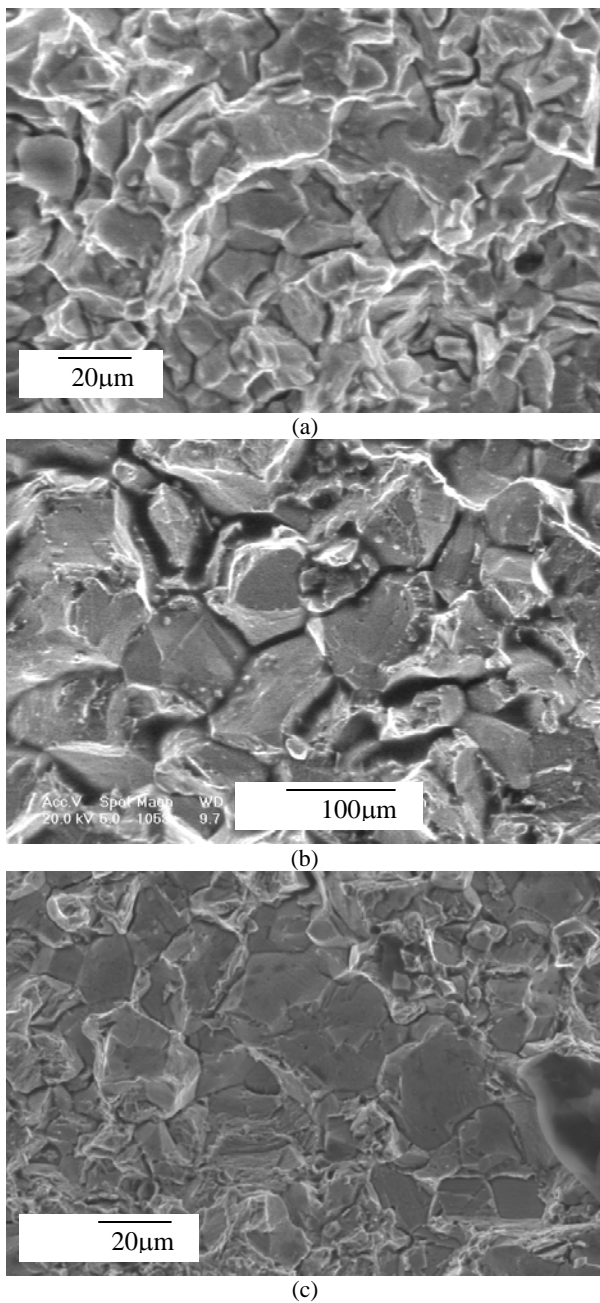


Figure 5: Fractographs of (a) X-750 AH, (b) X-750 HTH, and (c) 625 DA tested under room temperature hydrogenated conditions, showing intergranular fracture.

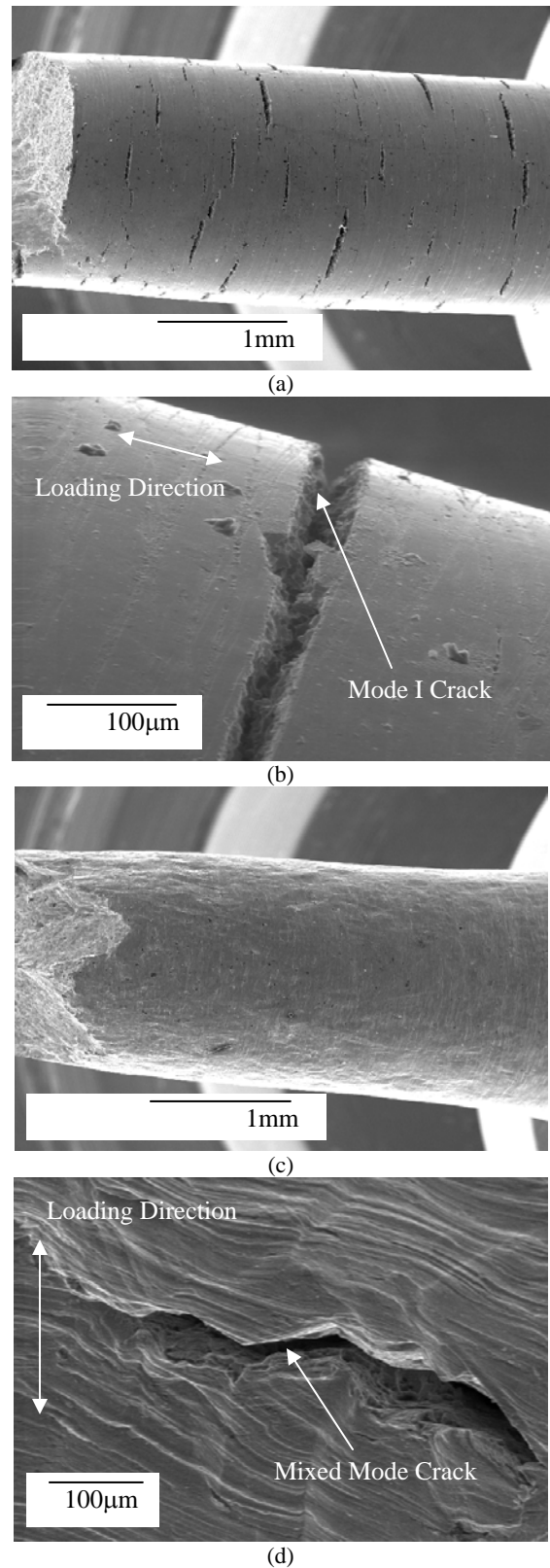


Figure 6: Surface deformation and cracking present on SSRT specimens failed at room temperature and tested under (a) and (b) hydrogenated conditions, as well as, (c) and (d) nitrogenated conditions.

conditions. Under all other test conditions (i.e., hydrogen free at room temperature and all tests at 150°C and 288°C), surface cracks were limited, and when they appeared they propagated in a mixed mode manner with large mode II in-plane shear displacements, as shown in Figure 6(d).

Examination of the data presented in this study is consistent with the findings of other researchers. In particular, it has been reported that these nickel-base alloys (among others) show two regimes of hydrogen embrittlement: (1) one that corresponds to reactor operating temperatures ($\geq 250^\circ\text{C}$) and (2) another at low temperatures ($\leq 150^\circ\text{C}$)^{9,10,13}. Especially in the low temperature regime, significant reductions in ductility occur and a brittle, intergranular fracture mode characterized by the propagation of a Mode I cracking has been observed. These observations suggest that these alloys may undergo premature failure during low temperature, hydrogenated reactor shutdown operations.

Conclusions

The hydrogen embrittlement susceptibilities of Alloy X-750 in the AH and HTH heat-treat conditions and Alloy 625 in the direct aged (DA) condition were determined at room temperature, 150°C, and 288°C in a simulated (out-of-flux) water reactor environment containing dissolved hydrogen gas (0 and 60 cc H₂/kg H₂O STP). The following conclusions can be drawn from this research:

- The three materials tested showed a pronounced susceptibility to hydrogen embrittlement at room temperature. The failure times and ductilities decreased by about 35% and 50%, respectively, when evaluated in hydrogenated versus nitrogenated environments.
- Further evidence of the room temperature hydrogen embrittlement susceptibility of these alloys included the transition from a ductile, transgranular fracture to a predominantly intergranular fracture path in the presence of dissolved hydrogen gas. The three materials tested exhibited an intergranular fracture, which was contiguous to the specimen surface and represented about 15% of the fracture surface.
- Surface cracking changed from mixed mode propagation inclined to the stress axis under nitrogenated tests to Mode I cracking, roughly normal to the stress axis, in the room temperature hydrogenated tests.
- At 288°C, none of the materials showed any hydrogen embrittlement. Ductile fracture due to microvoid coalescence occurred by cup-cone failure for the Alloy X-750 materials and Alloy 625 DA failed by ductile 45° shear. No intergranular fracture was observed. At 150°C, Alloy 625 DA showed some susceptibility to hydrogen embrittlement, which is consistent with the low temperature regime of susceptibility in these alloys reported by other researchers.
- The relative susceptibilities of these alloys to hydrogen embrittlement were indistinguishable. Especially in Alloy X-750, this observation implies that carbide precipitation does not affect hydrogen embrittlement, at least under our testing conditions. It remains to be seen whether Alloy 625 DA is superior to Alloy X-750 under irradiated tensile conditions.

Acknowledgements

We would like to thank Frank Loss and Robert Taylor of Materials Engineering Associates, Inc. for the use of their equipment and for their help in setting up the experiments. We

acknowledge helpful discussions with Doug Symons and Michael Lebo. We thank the staffs of Penn State's Center for Advanced Materials and Breazeale Nuclear Reactor.

References

1. P.L. Andresen et al., "State of Knowledge of Radiation Effects on Environmental Cracking in Light Water Reactor Core Materials" (Paper presented at the 4th International Symposium on Environmental Degradation of Materials in Nuclear Power Systems – Water Reactors, Jekyll Island, Georgia, 6 August 1989), 83.
2. P. Scott, "A Review of Irradiation Assisted Stress Corrosion Cracking," Journal of Nuclear Materials, 211, (1994), 101-122.
3. H. Hanninen and I. Aho-Mantila, "Environmental-Sensitive Cracking of Reactor Internals" (Paper presented at the 3rd International Symposium on Environmental Degradation of Materials in Nuclear Power Systems – Water Reactors, Traverse City, Michigan, 30 August 1987), 77.
4. O.K. Chopra et al., "Environmentally Assisted Cracking in Light Water Reactors" (Report NUREG/CR-4667 Vol. 23 ANL-97/10, Argonne National Laboratory, 1996).
5. "Standard Specification for Precipitation-Hardening Nickel Alloy Bars, Forgings, and Forging Stock for High-Temperature Service," ASTM Standard B637-93a (Philadelphia, PA: American Society for Testing Materials, 1993), 471-475.
6. C.A. Grove and L.D. Petzold, "Mechanisms of Stress-Corrosion Cracking of Alloy X-750 in High-Purity Water," (Paper presented at the International Conference on Corrosion of Nickel-Base Alloys, Cincinnati, Ohio, 23 October 1984), 165.
7. J.R. Donati et al., "Stress Corrosion Cracking Behavior of Nickel-Base Alloys with 19% Chromium in High Temperature Water" (Paper presented at the 3rd International Symposium on Environmental Degradation of Materials in Nuclear Power Systems – Water Reactors, Traverse City, Michigan, 30 August 1987), 697.
8. M.T. Miglin and H.A. Domian, "Microstructure and Stress Corrosion Resistance of Alloys X-750, 718, and A286 in Light Water Reactor Environments," Journal of Materials Engineering, 9 (2) (1987), 113-132.
9. C.A. Grove and L.D. Petzold, "Mechanisms of Stress-Corrosion Cracking of Alloy X-750 in High-Purity Water," Journal of Materials for Energy Systems, 7 (2) (1985), 147-162.
10. P. Skeldon, P.M. Scott, and P. Hurst, "Environmentally Assisted Cracking of Alloy X-750 in Simulated PWR Coolant," Corrosion, 48 (7) (1992), 553-569.
11. M.K. Miller and M.G. Burke, "An APFIM/AEM Characterization of Alloy X750," Applied Surface Sciences, 67 (1993), 292-298.
12. T. Yonezawa, Y. Yanaguchi, and Y. Iijima, "Electron Micro Autoradiographic Observation of Tritium Distribution on Alloy X750" (Paper presented at the 6th International Symposium on Environmental Degradation of Materials in Nuclear Power Systems – Water Reactors, San Diego, California, 1 August 1993), 799.
13. W.J. Mills et al., "Effect of Irradiation on the Stress Corrosion Cracking Behavior of Alloy X-750 and Alloy 625" (Paper presented at the 6th International Symposium

- on Environmental Degradation of Materials in Nuclear Power Systems – Water Reactors, San Diego, California, 1 August 1993), 633.
14. R. Bajaj et al., “Irradiation-Assisted Stress Corrosion Cracking of HTH Alloy X-750 and Alloy 625” (Paper presented at the 7th International Symposium on Environmental Degradation of Materials in Nuclear Power Systems – Water Reactors, Breckenridge, Colorado, 7 August 1995), 1093.
 15. P.D. Hicks and C.J. Altstetter, “Internal Hydrogen Effects on Tensile Properties of Iron- and Nickel-Base Superalloys,” Metallurgical Transactions A, 21 (1990), 365-372.
 16. P.D. Hicks and C.J. Altstetter, “Hydrogen-Enhanced Cracking of Superalloys,” Metallurgical Transactions A, 23 (1992), 237-249.
 17. B.G. Pound, “Hydrogen Trapping in Work-Hardened Alloys,” Acta Metallurgica et Materialia, 39 (9) (1991), 2099-2105.
 18. A.M. Brass and J. Chene, “Influence of Deformation on the Hydrogen Behavior in Iron and Nickel Base Alloys: A Review of Experimental Data,” Materials Science and Engineering A, 242 (1998), 210-221.
 19. G.S. Was, “Grain-Boundary Chemistry and Intergranular Fracture in Austenitic Nickel-Base Alloys – A Review,” Corrosion, 46 (4) (1990), 319-330.
 20. Y. Shen and P.G. Shewmon, “Intergranular Stress Corrosion Cracking of Alloy 600 and X-750 in High-Temperature Deaerated Water/Steam,” Metallurgical Transactions A, 22 (1991), 1857-1864.
 21. J. Yao, S.A. Meguid, and J.R. Cahoon, “Hydrogen Diffusion and its Relevance to Intergranular Cracking in Nickel,” Metallurgical Transactions A, 24 (1993), 105-112.
 22. D.M. Symons and A.W. Thompson, “The Effect of Hydrogen on the Fracture of Alloy X-750,” Metallurgical Transactions A, 27 (1996), 101-110.
 23. W.S. Walston, I.M. Bernstein, and A.W. Thompson, “The Effect of Internal Hydrogen on a Single-Crystal Nickel-Base Superalloy,” Metallurgical Transactions A, 23 (1992), 1313-1322.
 24. D.D. Macdonald et al., “Corrosion Studies on Alloy 182 in Simulated BWR Environments” (Final Report to Ishikawajima-Harima Heavy Industries Co., Ltd., The Pennsylvania State University Center for Advanced Materials, 1996).
 25. P. Skeldon and P. Hurst, “Environmentally Assisted Cracking of Inconel X750” (Paper presented at the 3rd International Symposium on Environmental Degradation of Materials in Nuclear Power Systems – Water Reactors, Traverse City, Michigan, 30 August 1987), 703.
 26. J.L. Hertzberg and G.S. Was, “Isolation of Carbon and Grain Boundary Carbide Effects on the Creep and Intergranular Stress Corrosion Cracking Behavior of Ni-16Cr-9Fe-xC Alloys in 360°C Primary Water,” Metallurgical and Materials Transactions A, 29 (1998), 1035-1046.